Korean J. Chem. Eng., 33(4), 1255-1260 (2016)
DOI: 10.1007/s11814-015-0283-8

pISSN: 0256-1115
eISSN: 1975-7220

Surface analysis of three aluminum foils and relation to hydrogen generation capability

Heidy Visbal†, Kohji Nagashima, and Kazuyuki Hirao

Faculty of Engineering, Kyoto University, A3-120 Kyoto Daigaku Katsura, Nishikyo-ku, Kyoto-shi, Kyoto 615-8510, Japan
(*Received 3 April 2015 • accepted 16 December 2015*)

Abstract−We have successfully generated hydrogen using aluminum foil instead of aluminum powder from the perspective of improving safety. We analyzed the surface states of three aluminum foils and correlated their surface properties with hydrogen generation capability. The surfaces of the foils were analyzed by time-of-flight secondary ion mass spectrometry (TOF-SIMS), X-ray photoelectron spectroscopy, and atomic force microscopy. Hydrogen generation was performed by adding $Ca(OH)_2$ solution to the aluminum foil in water. The TOF-SIMS results showed that the Al foils have $Al_2O_3^-$, AlO_2^-, $(OH)_2AlO^-$, $(Al_2O_3)OH^-$, and $(Al_2O_3)AlO_2^-$ and related species on their surfaces. The amount of these species on the surface of an Al foil is linearly correlated with the hydrogen generation reaction rate.

Keywords: Hydrogen Generation, Aluminum Foil, TOF-SIMS

INTRODUCTION

As a clean energy carrier hydrogen is regarded as a potential alternative to fossil fuels [1]. However, its wide use is limited by problems associated with its storage and transportation [1-3]. Moreover, a safe and low-cost hydrogen generation technique is desirable. In general, hydrogen is mainly produced in large quantities by the steam reforming of hydrocarbons such as methane, but this process is not environmentally friendly. Hydrogen can also be produced by chemical hydrides reacting with water [4-6], splitting water using a metal oxide catalyst [7-9], and corrosion of base metals such as aluminum in solutions [10-12].

Aluminum is a promising hydrogen generating material because it has a relatively low price (less than 2$/kg), and 1 kg of Al reacting with water produces 0.11 kg of hydrogen. It costs $18 per kg of hydrogen and it can be reduced by using aluminum from recycle cans.

It can be stored and transported in a much safer and more convenient manner than hydrogen [13].

In the literature, alumina films on the surface of aluminum are reported to act as a protective barrier layer and can inhibit the aluminum-water reactions [13,14-16]. Understanding how an alumina film can inhibit hydrogen generation and correlating the surface structure of aluminum with hydrogen generation is important.

Most studies on hydrogen generation from aluminum are based on powder reactions. However, aluminum powder is very reactive and may cause dust explosions. This process has very practical limitations. To avoid violent reactions or explosions, we investigated the generation of hydrogen using an aluminum foil instead of aluminum powder from the perspective of improving safety [17] and to reduce cost in the future if we use aluminum from recycle sources.

†To whom correspondence should be addressed.
E-mail: visbal.heidy.2x@kyoto-u.ac.jp

We analyzed the surface states of three aluminum foils and correlated their surface properties with the hydrogen generation capability. The surfaces of the foils were analyzed by time-of-flight secondary ion mass spectrometry (TOF-SIMS), X-ray photoelectron spectroscopy (XPS), and atomic force microscopy (AFM).

Commonly, many authors simply describe the oxide structure of aluminum surface as alumina or with the general formulae Al_2O_3. Concerning the chemical structure of the oxide, the chemical structure and the local environment of aluminum atoms in the oxide are not correlated with generation of hydrogen until now.

TOF-SIMS is capable of providing detailed information of chemical and molecular structure of the surfaces. The technique consists of bombarding the sample with a pulsed primary ion beam with a dose $<1\times10^3$ atoms cm^{-2}. It has a high detection limit (<10 ppm) and high lateral resolution (0.2 μm).

Our aim was to show the utility of TOF-SIMS in analyzing the thin oxide passive film and the structure in details on three different aluminum foils surface and its relation with hydrogen generation capability.

EXPERIMENTAL

Three aluminum foils, Japanese Industrial Standards (JIS) grade, were supplied from UACJ Corporation in Japan. $Ca(OH)_2$ was purchased from NACALAI TESQUE, INC. as an extra pure reagent (>95.0%). $Ca(OH)_2$ powder was added to remove the surface oxide and ignite the hydration reaction of an aluminum foil. According to manufacturer's data, all aluminum foils used contained less than 2% foreign metals (Fe, Cu, Zn, Si, and so on). The chemical compositions of the three Al foils used are summarized in Table 1.

To remove paraffin coating or any organic coating layer, the foils were rinsed with ethanol, hexane, and acetone each for 5 min. A mixture of 1 g of an aluminum foil cut into small pieces of 25×25 mm^2 and thickness of 12 μm and 1 g of $Ca(OH)_2$ powder was placed in a 500 ml flask, and then 300 ml of distilled water was

Table 1. Chemical compositions of the three aluminum foils

Material	Thickness (μm)	Chemical composition (9%)					Conversion yield (%)
		Si	Fe	Cu	Zn	Al	
1N30	12	Si+Fe 0.70		0.10		99.20	91
8021	12	0.15	1.2 1.7			98.15	73
8079	12	0.05 0.30	0.70 1.30		0.10	98.30	64

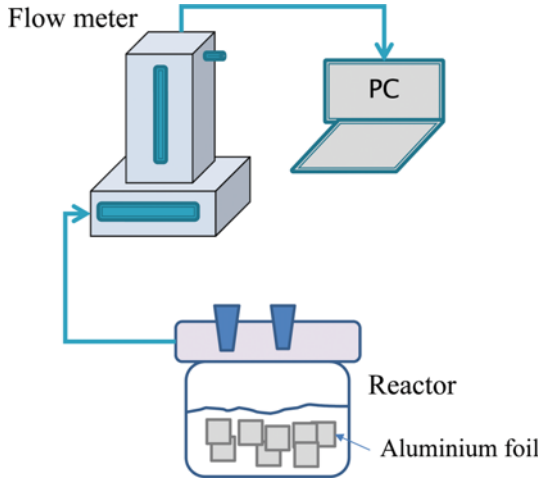

Fig. 1. Schematic of the hydrogen generation system.

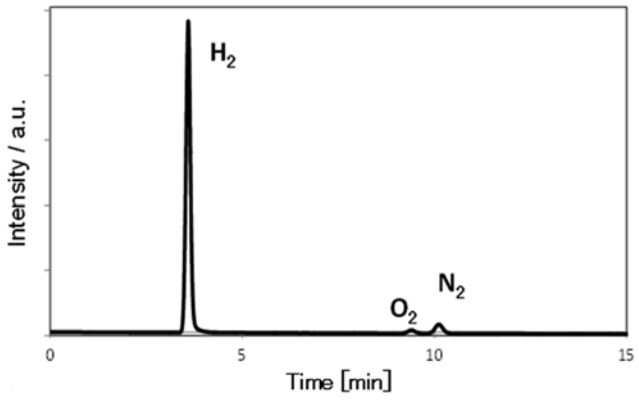

Fig. 2. Gas chromatography results of the gas generated by the reaction of aluminum foils and water.

added. The flow rate and total amount of generated gas was monitored using a high precision film flow meter on a HORIBA STEC VP-2U. The components of the produced gas were analyzed by gas chromatography using a Shimadzu GC-2014 equipped with a SHINCARBON ST column (6 m). Fig. 1 shows a schematic of the measurement system of hydrogen generation.

SURFACE CHARACTERIZATION

Surface analysis was performed using a TOF-SIMS TRIFT IV nano-TOF (ULVAC PHI, Japan). Static SIMS with an ion dose of less than 1×10^{12} ions·cm^{-2} was employed using 30 keV Au^{3+} gold trimer ion beam at a current of 3 nA, operating in the high current bunched mode, at a pulse width of 18.0 ns. The analysis area was 100×100 μm^2. Spectra were acquired over a mass range of 0-1,800 u in both the positive and negative ion modes. Fragments of known composition such as H^+, CH_3^+, and OH^- were used for mass calibration.

The intensities for particular fragment ions under consideration were evaluated using the concept of their relative peak intensity (RPI), which is the ratio of the intensity of the ion of interest relative to the total ion intensity from m/z=0-1,800 u.

$$RPI_x = I_x / I_{totab}$$

where x is the ion of interest, I_{total} is the total ion intensity between m/z=1 and 1,800 u, and I_x is the measured intensity of the ion under consideration [18].

XPS measurements were performed on a PHI 5000 VersaProbe (ULVAC-PHI) with monochromatic Al Kα (1.4866 keV).

The surface morphology was visualized by AFM (AIST, Co.) in the intermittent contact mode using Olympus OMCL-160TS cantilevers. The RMS roughness for each group of samples was calculated as an average value of the measurements performed over three areas on each sample.

RESULTS AND DISCUSSION

1. Hydrogen Generation Results

Fig. 2 shows the results of gas chromatography during the hydrogen generation reaction for 1N30. The strong peak at 3.6 min, the small dips at 9.6 min, and the small dips at 11.1 min in the retention time show hydrogen, oxygen, and nitrogen, respectively. The produced gas detected during the reaction was identified as hydrogen. The N_2 and O_2 peaks are due to the mixture of residual air from the glass flask. For the three foils, the detected gas was hydrogen.

Fig. 3 shows the result of the total amount of hydrogen generation of the three aluminum foils. The generation rate of hydrogen can be observed to be around 2 h for all samples, but the yield of hydrogen obtained differs with the aluminum foil used. The hydrogen yield is calculated based on the theoretical amount of hydrogen generated by Al and water.

The Al foil defined as 1N30 showed a hydrogen yield of 97%, and aluminum 8021 and 8079 showed a yield of 76% and 67%,

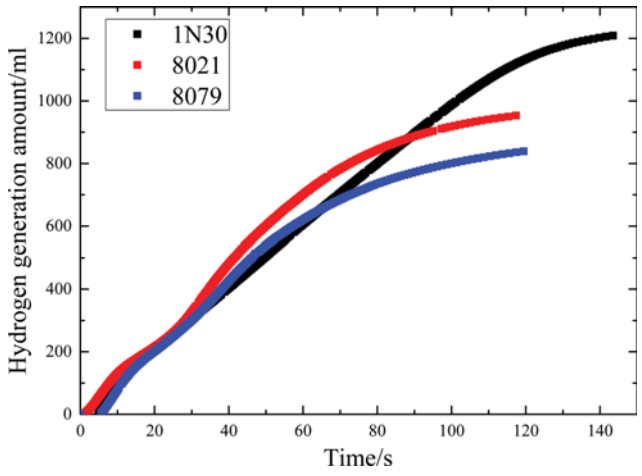

Fig. 3. Hydrogen generation amount of the three aluminum foils.

respectively. The data together with the chemical composition of each aluminum foil are summarized in Table 1. Although the 1N30 foil has a lesser amount of foreign metals, there is no direct relation between the amounts of these metals with hydrogen generation. For example, 8021 has more metals than 8079, but the hydrogen generation yield is smaller in the case of the 8079 sample. This demonstrated that the surface composition, more than foreign metals in the chemical composition of the aluminum foil, plays a more important role in the hydrogen generation mechanism.

To elucidate the surface composition, we discuss the results obtained by TOF-SIMS, XPS, and AFM as follows.

2. TOF-SIMS Results

TOF-SIMS has been used for elemental depth profiling for more than 30 years [19]. It allows a unique assignment of the composition of the secondary ions encountered in a contaminated oxidized aluminum surface. The negative SIMS spectrum for Al(1N30) is presented in Fig. 4. Over the mass range of 0-180, several peaks are detected. Among all the peaks, signals originating from the aluminum oxide layer were taken from SIMS database [20] as follows: 16 (O^-), 59 (AlO_2^-), 77 ($AlO(OH)_2^-$), 119 ($[Al_2O_3(OH)]^-$), and 161 [$(Al_2O_3)AlO_2^-$]. Additionally, cluster ions or aluminum in other oxides structure were detected like [$Al_2O_3^-$]. The completed list is presented in Table 2.

Table 2. Aluminum oxide related fragment ions for each sample and its normalized intensity value

Fragmention	m/z	8079	8021	1N30	R^2
AlO^-	43	102.68	98.63	61.54	0.9101
$AlOH^-$	44	3.54	2.9	2.27	0.9821
AlO_2^-	59	70.58	65.1	38.71	0.9496
$AlO(OH)^-$	60	7.93	6.98	4.42	0.9834
AlO_3^-	75	3.19	2.86	2.96	0.3353
$AlO_2(OH)^-$	76	4.6	3.95	2.33	0.9875
$AlO(OH)_2^-$	77	7.6	4.98	4.59	0.7411
$Al(OH)_3^-$	78	1.21	1.43	0.76	0.5633
$Al(OH)_4^-$	95	0.85	0.62	0.59	0.7289
$Al_2O_3^-$	102	3.85	3.3	2.21	0.9966
$Al_2O_4^-$	118	2.25	1.66	1.16	0.9689
$Al_2O_3OH^-$	119	14.54	10.32	9.3	0.796
$Al_2O_2(OH)_3^-$	137	1.26	0.71	1.2	0.0009
$Al_2O_3(AlO)^-$	145	2.23	2.02	2.06	0.4519
$Al_2O_3(AlO_2)^-$	161	2.37	1.88	1.49	0.9624
$Al_2O_3Al_2O(OH)_2^-$	179	2.62	1.65	2.23	0.0771

Other signals different from oxide layer were identified but not listed here as their contribution to the present study is not significant. Their assignment corresponds to surface contamination of hydrocarbon compounds or oxides of foreign metals other than aluminum: For example, 121 ($Al_3C_2O^-$), 137 ($CH_2O_6Al^-$). We discuss here only the aluminum native oxide related peaks.

Fig. 5 shows four fragment ions from the SIMS database related to the oxide layer for the three aluminum foils studied. The quantification was made using the concept of their relative peak intensity (RPI), as explained in the experimental procedure and presented in Table 2 for all the peaks studied in this work.

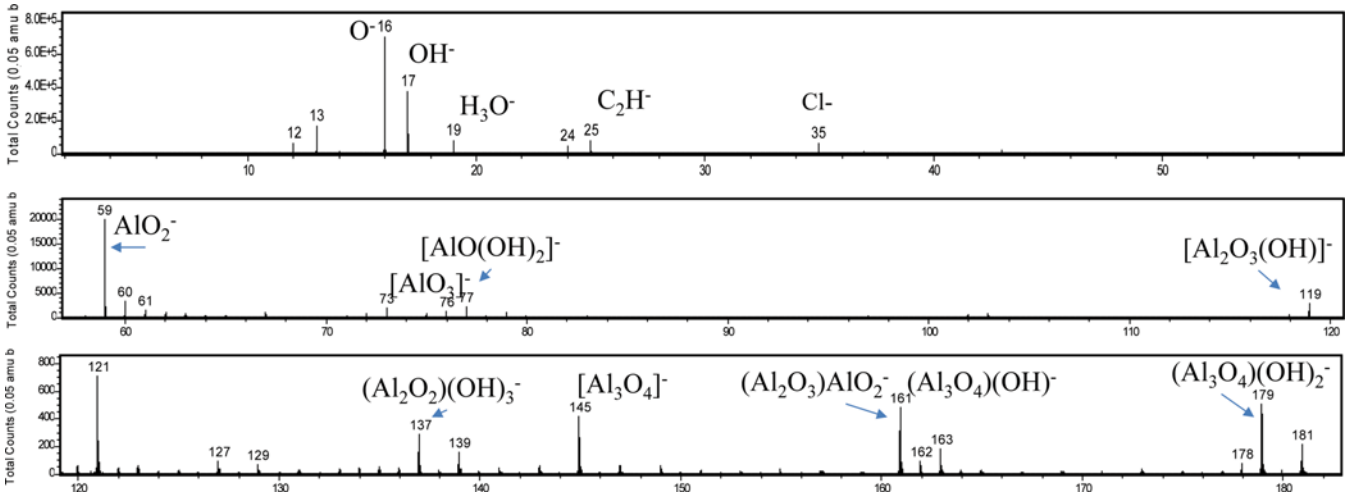

Fig. 4. The negative SIMS spectrum for the Al(1N30) sample.

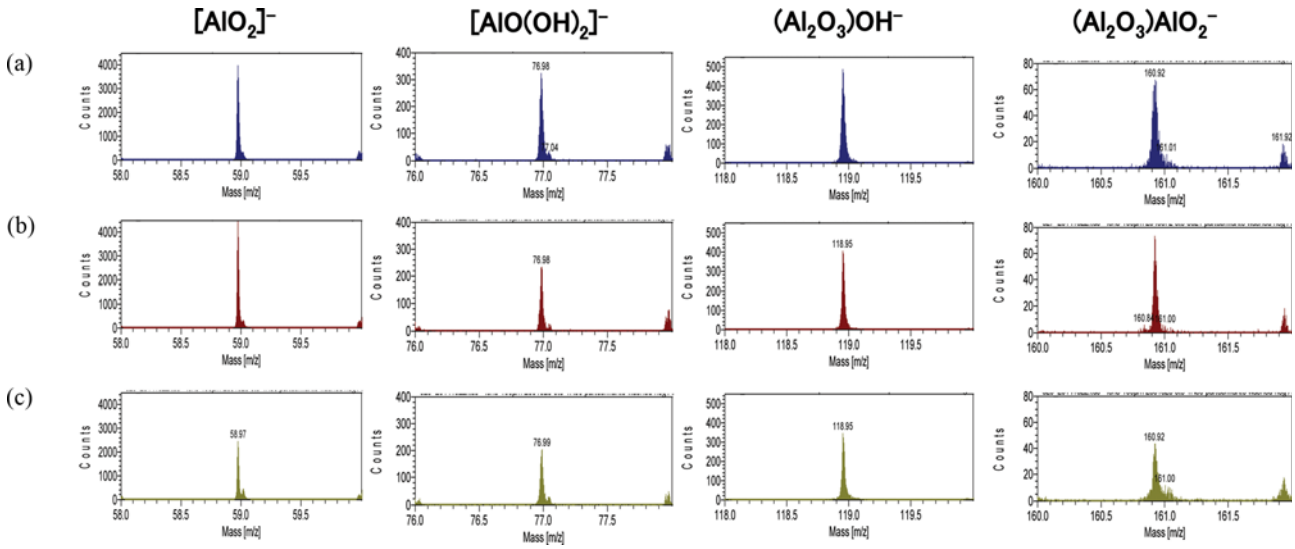

Fig. 5. Fragment ions related to the oxide layer at the aluminum surface. (a) Al(8079), (b) Al(8021), (c) Al (1N30).

As observed in Table 2, the sample Al(8079) shows a greater amount for oxide related fragment ions compared with the other two samples (8021, 1N30). Each fragment ion was plotted vs hydrogen generation yield. In Fig. 6 are plotted the fragment ions that showed best correlation with hydrogen generation yield. The best linear correlation (R=0.9966) was found for $Al_2O_3^-$ fragment ion followed by $AlO_2(OH)^-$, $AlO(OH)^-$, $AlOH^-$, $Al_2O_4^-$, $Al_2O_3(AlO_2)^-$ ions, which also showed a high correlation value of $R^2 \geq 0.96$. The R^2 value of correlations curve can be found in Table 2 for all the peaks analyzed in this study.

Fig. 6 shows clearly that the more fragment ion intensity found it was a high correlation with hydrogen generation yield. Also, some aluminum oxide cluster identified like m/z=179 does not show a clear relationship with the hydrogen generation yield. This indicates that small cluster oxide groups present at the surface of aluminum did not react or inhibited the reaction of hydrogen gen-

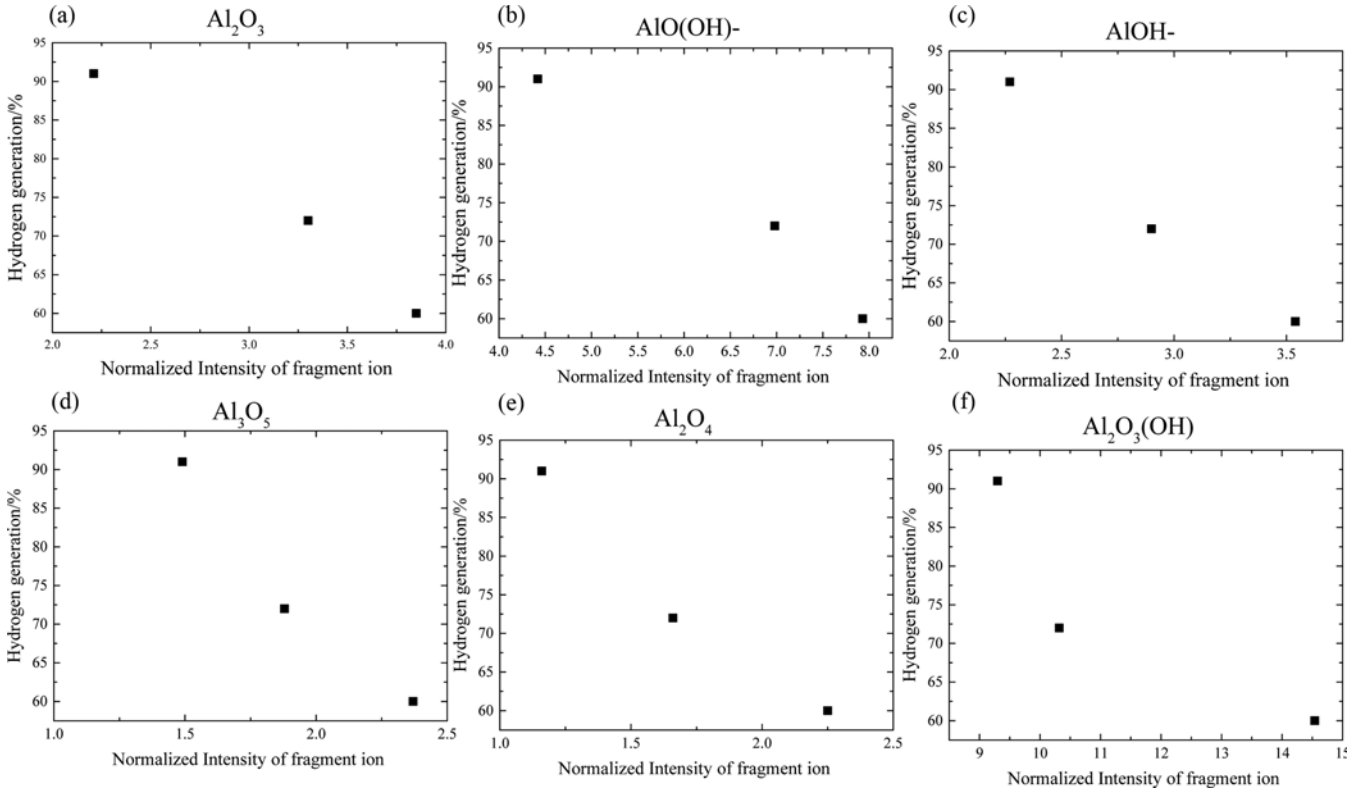

Fig. 6. Normalized intensity of aluminum oxide negative fragment ions and relation with the hydrogen generation yield.

Table 3. Atomic concentration of the three aluminum foils determined by XPS

Atomic concentration/%							
	Cls	Ols	Al2p	Na1s	Mg2p	Al/O	Al^0/Al^{3+}
1N30	27.33	48.02	24.65			0.51	75.7
8021	27.35	46.95	24.01	0.76	0.92	0.51	80.1
8079	27.11	46.74	23.97	0.75	1.26	0.51	92.4

eration directly. The reason for this behavior could be the amount of those groups at the surface of the facility to react or be attacked by the Ca^{2+} ion or OH^- ion in the system, as explained later.

TOF-SIMS results showed that the composition of native layer oxide at the aluminum surface plays a straightforward role in hydrogen generation in this system.

3. XPS Results

To elucidate the elemental surface composition of the three aluminum foils, XPS analyses were performed. The surface compositions of the three aluminum foils obtained by XPS are shown in Table 3. The samples exhibit a relatively high carbon concentration derived from impurities but not significant variations derived from the samples. The ratio of Al2p/O1s also does not show any variation with respect to the nature of the aluminum foil.

The Al 2p spectra (Fig. 7(a)) show two peaks corresponding to Al^0 and Al^{3+}, and the peak fit results are shown in Table 3. The Al 2p (metal) signal diminishes when an unstable oxide film is converted to a thickened hydroxide layer. As can be observed, the sample 1N30 shows a lower amount of this hydroxide layer at the aluminum surface.

The relation between the aluminum oxide percentage and hydrogen generation yield obtained by XPS can be observed in Fig. 7(b). As aluminum oxide percentage increases, the hydrogen generation yield decreases. However, this correlation is not linear as compared with the relationship with the aluminum oxide surface fragment determined by TOF-SIMS (Fig. 6). This result indicates that the amount of oxide (hydroxide) layer on the surface of an aluminum foil is an important factor in the hydrogen reaction system, but the nature composition of the oxide layer, like ($[Al_2O_3^-]$, $[AlO_2^-]$, $[AlO(OH)_2^-]$, $[Al_2O_3(OH)^-]$, and $[(Al_2O_3)AlO_2^-]$) surface groups is more important, as we discuss in TOF-SIMS analysis.

4. AFM Results

For imaging and analyzing the surface topography of the aluminum surface, AFM analysis was used. The root mean square (rms) surface roughness of the aluminum foils is presented together with the AFM image in Fig. 8. The rms values are 0.034, 0.096, and 0.056

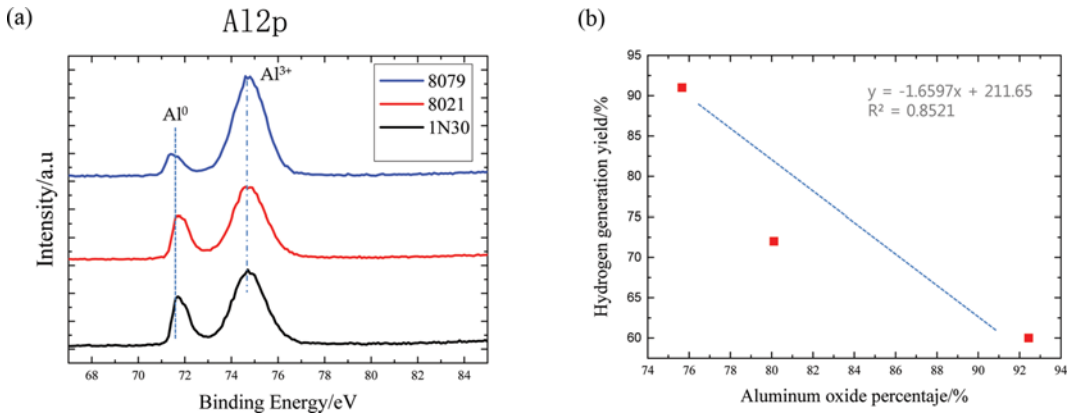

Fig. 7. (a) Al 2p photoelectron spectra of the three aluminum foils, (b) correlation between the aluminum oxide percentage (Al^0/Al^{3+}) from the Al 2p peak fit and hydrogen generation yield.

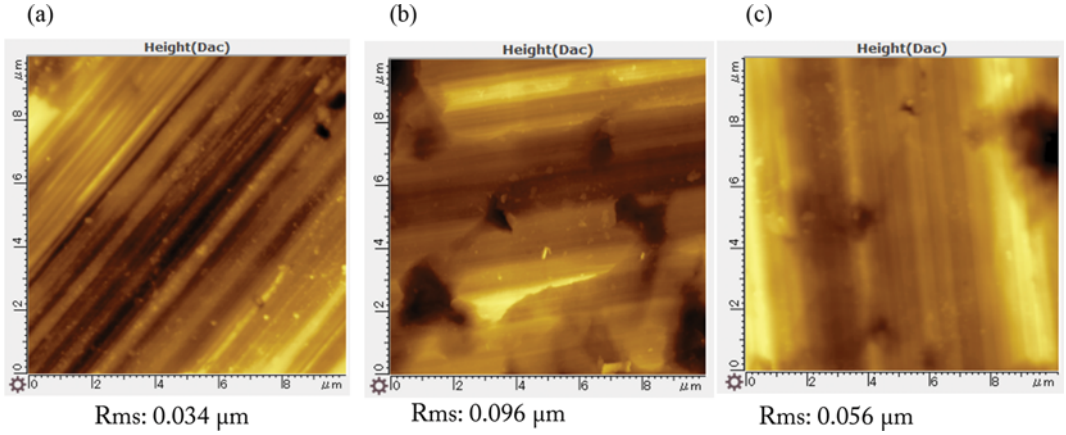

Fig. 8. Surface topography of the aluminum foils (a) 1N30, (b) 8021, (c) 8079.

mm for Al(1N30), Al(8021), and Al(8079), respectively. The sample Al(1N30) has a smaller surface roughness compared with the other two samples. Normally, surfaces with high surface roughness show more reactivity, but it is not applicable in this case. There is no direct relation between the surface roughness (rms value) and hydrogen capability of the aluminum foils, indicating that surface roughness does not directly influence the hydrogen generation yield.

5. Discussion

It is widely known that metal aluminum presents a dense oxide layer on its surface and that this layer inhibits the aluminum hydrolysis reaction. In this study, the corrosion resistance of aluminum is critically dependent not only on the presence of the passive oxide film that is formed on its surface, but also on the surface groups (fragments ions) detected by TOF-SIMS such as $Al_2O_3^-$, AlO_2^- and $Al_2O_3(OH)^-$.

The basic possible aluminum oxidation reactions in water are as follows:

$$Al+3H_2O \rightarrow Al(OH)_3+3/2H_2 \quad (1)$$

$$Al+2H_2O \rightarrow AlOOH+3/2H_2 \quad (2)$$

$$Al+3/2H_2O \rightarrow 1/2Al_2O_3+3/2H_2 \quad (3)$$

$$Al_2O_3+H_2O \rightleftarrows 2AlOOH \quad (4)$$

$$AlOOH+H_2O \rightleftarrows Al(OH)_3 \quad (5)$$

$$Al(OH)_3+OH \rightleftarrows Al(OH)_4^- \quad (6)$$

$$3Ca^{2+}+2Al(OH)_4^-+8H_2O \rightleftarrows Ca_3Al_2(OH)_{12}+6H_2 \quad (7)$$

The details of the mechanism of these reactions are discussed in our previous study [21]. In reactions (1)-(3), all reactions are accompanied by the release of hydrogen and solid byproducts such as bayerite [$Al(OH)_3$], boehmite [$AlO(OH)^-$], and aluminum oxide [Al_2O_3]. However, in reaction (7), the subproducts also react to generate hydrogen. The existence of different aluminum oxide groups implies a different induction time for the beginning of the reaction and that these groups could react with the system and inhibit hydrogen generation. After the induction time, hydrogen generation is controlled by the reaction between the oxygen surface groups and calcium ions in water.

In this study, we have shown the utility and high sensitivity of TOF-SIMS in analyzing thin oxide passive films on an aluminum surface and its relation with hydrogen generation capability.

Compared with XPS, TOF-SIMS results showed that the nature of the surface oxide groups at the surface becomes a very important factor in the hydrogen generation yield, and a detailed study of these groups could help to elucidate reactions at the aluminum surface to generate hydrogen.

CONCLUSIONS

Three aluminum foils were used to react with water and $Ca(OH)_2$ under ambient conditions. The surface properties of these foils were related to hydrogen generation capability. XPS results showed a passive oxide film for all three aluminum foils, but the amount varied depending on the aluminum foil used. It was determined by TOF-SIMS that the oxygen-related surface groups $Al_2O_3^-$, $AlOO^-$ and $Al_2O_3(OH)^-$ and their amount on the aluminum surface correlate linearly with the hydrogen generation capability. No relation was found between surface roughness and hydrogen generation. The reaction of aluminum with water is controlled by the surface chemical reaction at the initial stage and then by the reaction between the oxygen surface groups and calcium ions for the corrosion reaction of aluminum. We showed the utility and high sensitivity of TOF-SIMS in analyzing thin oxide passive film on the aluminum surface and its relation to hydrogen generation capability.

REFERENCES

1. X. Huang, C. Lu, Y. Huang, S. Liu, C. Wang and D. Chen, *Int. J. Hydrogen Energy*, **36**, 15119 (2011).
2. A. V. Parmuzina and O. V. Kravchenko, *Int. J. Hydrogen Energy*, **33**, 3073 (2008).
3. O. V. Kravchenko, K. N. Semenenko, B. M. Bulychev and K. B. Kalmykov, *J. Alloys Compd.*, **397**, 58 (2005).
4. M. M. H. Bhuiya, A. Kumar and K. J. Kim, *Int. J. Hydrogen Energy*, XXX, **I-I7** (2014).
5. Y. Kojima, K. Suzuki, K. Fukumoto, M. Sasaki, T. Yamamoto and Y. Kawai, *Int. J. Hydrogen Energy*, **27**, 1029 (2001).
6. B. P. Tarasov, V. V. Burnasheva, M. V. Lototskiy and V. A. Yartys, *Int. Sci. J. Alternative Energy Ecol. ISJAEE*, **12**, 14 (2005).
7. A. Fujishima and K. Honda, *Nature,* **238**, 37 (1972).
8. R. van de Krol, Y. Liang and J. Schoonman, *J. Mater. Chem.*, **18**(20), 2311 (2008).
9. C. Li, J. Yuan, B. Han, L. Jiang and W. Shanguan, *Int. J. Hydrogen Energy*, **35**, 7073 (2010).
10. D. Belitskus, *J. Electrochem. Soc.*, **117**, 1097 (1970).
11. L. Soler, J. Macana, M. Munoz and J. Casado, *Int. J. Hydrogen Energy*, **32**(18), 4702 (2007).
12. A. V. Parmuzina and O. V. Kravchenko, *Int. J. Hydrogen Energy*, **33**, 3073 (2008).
13. W. Gai, W. Liu, Z. Deng and J. Zhou, *Int. J. Hydrogen Energy*, **37**, 13132 (2012).
14. X. Huang, T. Gao, X. Pan, D. Wei, C. Lv, L.Qin and Y. Huang, *J. Power Sources*, **229**, 133 (2013).
15. B. Alinejad and K. Mahmoodi, *Int. J. Hydrogen Energy*, **34**, 7934 (2009).
16. P. Dupiano, D. Stamatis and E. L. Dreizin, *Int. J. Hydrogen Energy*, **36**, 4781 (2011).
17. K. Nagashima, H. Visbal, S. Kanehira, T. Saeki, R. Chinzaka, M. Shimizu, M. Nishi and K. Hirao, to be submitted.
18. K. Shimizu, C. Phanopoulos, R. Loenders, M. Abel and J. Watts, *Surf. Interface Anal.*, **42**, 1432 (2010).
19. E. Niehuis and T. Grehl, in ToF-SIMS: Surface Analysis by Mass Spectrometry, (Eds: J. C. Vickerman, D. Briggs), IM Publications and Surface Spectra Limited, Chichester, **2001**, 753.
20. The Static SIMS Library, Editors: J. C. Vickerman, D. Briggs, A. Henderson (2012).
21. S. Kanehira, S. Kanamori, K. Nagashima, T. Saeki, H. Visbal, T. Fukui and K. Hirao, *J. Asian Ceram. Soc.*, **1-3**, 296 (2013).